ChemComm

Cite this: *Chem. Commun.*, 2011, **47**, 8361–8363

www.rsc.org/chemcomm

COMMUNICATION

Synthesis of anatase TiO_2 rods with dominant reactive {010} facets for the photoreduction of CO_2 to CH_4 and use in dye-sensitized solar cells†

Jian Pan,[a] Xia Wu,[b] Lianzhou Wang,[b] Gang Liu,*[a] Gao Qing (Max) Lu[b] and Hui-Ming Cheng[a]

Received 24th May 2011, Accepted 13th June 2011
DOI: 10.1039/c1cc13034j

Single crystalline anatase TiO_2 rods with dominant reactive {010} facets are directly synthesized by hydrothermally treating $Cs_{0.68}Ti_{1.83}O_4/H_{0.68}Ti_{1.83}O_4$ particles. The nanosized rods show a comparable conversion efficiency in dye-sensitized solar cells (DSSCs), and a superior photocatalytic conversion of CO_2 into methane to the benchmark P25 TiO_2 nanocrystals.

Photocatalysis is a promising process to convert solar energy.[1] A high percentage of reactive facets in photocatalysts by crystal facet engineering has been actively pursued due to the competitive advantages in optimizing photocatalytic reactivity and/or selectivity.[2] Faceting an anatase TiO_2 photocatalyst has attracted increasing interest since a large percentage of high-energy {001} facets was realized.[3] Very recently, it has been reported that {010} with both a favorable surface atomic structure and surface electronic structure is most reactive among low index facets {001}, {010} and {101}.[4] Although the surface energy of {010} (0.53 J m^{-2}) is theoretically determined to be slightly higher than that (0.44 J m^{-2}) of {101} and much lower than that (0.90 J m^{-2}) of {001}, it is surprising that no {010} appears in the equilibrium shape of anatase.[5a] On the other hand, a couple of experimental studies have validated the possibility of growing {010} dominant anatase by using a correct organic or inorganic morphology controlling agent.[4,5b] An alternative route to prepare {010}-rich anatase was to hydrothermally treat pre-synthesized sodium titanate nanotubes without any morphology controlling agent in a basic solution environment.[6] The origin of stabilization of {010} facets is that *O*-terminated {010} has a lower surface energy than *O*-terminated {101} and {001} in the basic environment, which provides a powerful mechanism for growing {010} dominant anatase.[7] In this work, we showed that {010} dominant anatase rods can directly grow from lepidocrocite-type titanate particles. Due to the unique surface atomic/electronic structure, the nanosized rods show a superior activity in converting CO_2 into CH_4 and a comparable energy conversion efficiency as a working electrode in DSSCs to the benchmark P25 TiO_2 nanocrystals.

Lepidocrocite-type bulk titanate $Cs_{0.68}Ti_{1.83}O_4$ powder was prepared according to the previously reported solid state reactions.[8] Its protonated form $H_{0.68}Ti_{1.83}O_4$ was obtained by ion-exchange in 1 M chloric acid solution. The morphology of both $Cs_{0.68}Ti_{1.83}O_4$ and $H_{0.68}Ti_{1.83}O_4$ particles with a size of several hundreds of nanometres is irregular (see Fig. S1, ESI†). By hydrothermally treating $Cs_{0.68}Ti_{1.83}O_4$ powder in an aqueous solution at 180 °C for 24 h, all irregular particles disappeared and uniform rods with tetragonal sides and slightly truncated pyramid ends are formed as shown in Fig. 1a. X-Ray diffraction patterns in Fig. S2 (ESI†) confirm that these micrometre-sized rods are anatase TiO_2 (space group: $I4_1/amd$, JCPDS No. 21-1272). With $H_{0.68}Ti_{1.83}O_4$ as a precursor and Cs_2CO_3 as a pH mediator agent, nanosized

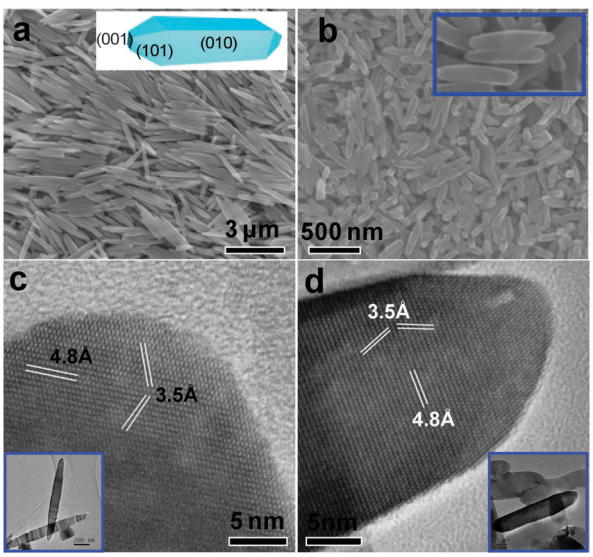

Fig. 1 SEM and HRTEM images of (a) micron-sized and (b) nanosized TiO_2 rods. The insets in (a) and (b) show a schematic shape of an anatase rod with {010}, {101}, {001} and a high-magnification SEM image of nanosized TiO_2 rods. The insets in (c) and (d) are the low-magnification TEM images of the micron- and nanosized rods.

[a] *Shenyang National Laboratory for Materials Science, Institute of Metal Research, Chinese Academy of Sciences, 72 Wenhua Road, Shenyang 110016, China. E-mail: gangliu@imr.ac.cn; Fax: +86 24 23903126; Tel: +86 24 83978238*
[b] *ARC Centre of Excellence for Functional Nanomaterials, School of Engineering and Australian Institute of Bioengineering and Nanotechnology, The University of Queensland, Qld. 4072, Australia*
† Electronic supplementary information (ESI) available: Sample preparation, XRD, XPS, Raman data, SEM images, performance tests. See DOI: 10.1039/c1cc13034j

anatase rods with a similar shape to that from $Cs_{0.68}Ti_{1.83}O_4$ are formed (see Fig. 1b). To identify the exposed facets of the rods, high resolution (HR) transmission electron microscopy (TEM) was used to reveal surface atomic structures. The HRTEM images in both Fig. 1c and d, recorded along the [001] direction of micro- and nanosized rods, give three sets of lattice fringes with spacings of 4.8, 3.5 and 3.5 Å, which are assigned to {002}, {101} and {10$\bar{1}$} facets, respectively. Clearly, the surface of these well faceted rods can be identified as lateral {010}, {101} and top {001} (see the inset in Fig. 1a), according to the SEM and TEM images together with the crystallographic symmetries of anatase.

The compositions of the rods and their states were investigated with X-ray photoelectron spectroscopy (XPS) and Raman spectroscopy. A number of Cs^+ ions were present in the rods as seen by the obvious XPS signal of Cs 3d in Fig. S3 (ESI†). These ions can be easily removed by a simple ion-exchange process with protons and subsequent calcination in air. Both the crystal phase and morphology of the rods show no detectable change after the above treatment. Prior to the removal of Cs^+, the binding energy of Ti 2p and O 1s is, however, shifted to a higher energy. An additional peak at *ca.* 532 eV is also seen in the O 1s XPS spectrum as a result of the presence of surface terminated Cs–O bonds. After the treatment, the binding energy of both Ti $2p_{3/2}$ and O 1s is shifted to 458.3 and 529. 5 eV, comparable to the previously reported values in clean anatase TiO_2.[9] The possible influence of the Cs^+ adsorption and surface treatment process on surface atomic structures was estimated by Raman spectroscopy. Different from the substantial role of surface terminated Ti–F bonds in affecting B_{1g} and A_{1g} modes,[10] the surface Cs–O bonds do not exert an obvious influence on the Raman active modes of anatase as shown in Fig. S4 (ESI†), suggesting that the surface atomic structure of anatase is well retained.

The combination of UV-visible absorption spectra with XPS valence band spectra of caesium-free anatase rods was used to determine electronic band alignments. As shown in Fig. 2a, in contrast to the micro-sized rods, the intrinsic absorption edge of the nano-sized rods has a blue-shift of 4 nm. The derived bandgap from the plots of the transformed Kubelka–Munk function *vs.* the energy of light is 3.27 and 3.32 eV for the micro-sized and nano-sized rods, respectively. The marginally larger bandgap of the nano-sized rods is apparently not caused by the quantum size effect because the critical size of TiO_2 is extremely small (5 nm). In the previous work,[4,10] it has been verified that {001} has a smaller bandgap than both {101} and {010} due to substantially different atomic configurations on each surface, and {010} has a bandgap close to {101}. Therefore, the rational reason for the bandgap difference between the two kinds of rods may be inferred to be a slightly higher percentage of {001} facets in the micro-sized rods. According to the valence band (VB) spectra in Fig. 2b, the VB maxima of both rods are at 1.96 eV, which is consistent with the reported value (1.93 eV) of {010} dominant anatase single crystals.[4] The unchanged VB maximum therefore indicates that the conduction band (CB) minimum of the nano-sized rods is raised by 0.05 eV with respect to the micro-sized rods (by *ca.* 0.12 eV compared to conventional anatase with a bandgap of 3.2 eV). The determined bandgap, CB minimum and VB maximum are given in Fig. 2c.

Anatase TiO_2 is the most widely investigated semiconductor serving as an electron collector to support a molecular sensitizer in dye-sensitized solar cells (DSSCs),[11] while TiO_2 crystals with well-defined facets are seldom investigated.[12] Here, we explore the possible advantages of {010} facets in DSSC applications as indicated in Fig. 3a and b. Due to the small specific surface area (4 m^2 g^{-1}) of the micro-sized rods and thus a limited dye adsorption ability, the micro-sized rod working electrode gives a quite low short-current (J_{sc}) of 4.2 mA cm^{-2} and solar energy conversion efficiency (η) of 1.72%. However, it is interesting to find that the nano-sized rods can substantially improve J_{sc} and η up to 16.5 mA cm^{-2} and 7.73%, respectively. These values are comparable to those

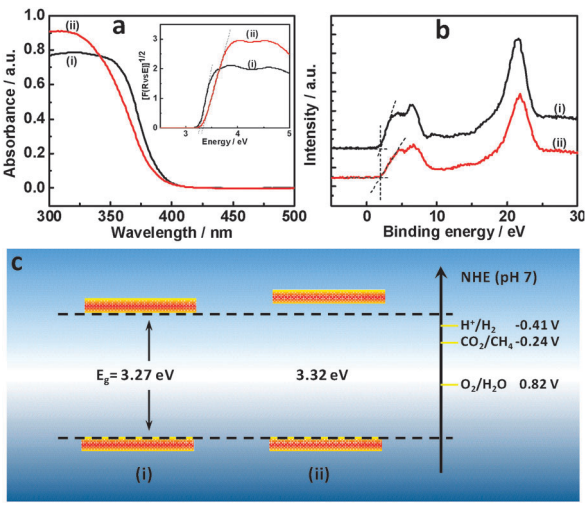

Fig. 2 (a) UV-visible absorption spectra; (b) XPS valence band spectra; (c) schematic of electronic band alignments of caesium-free micro-sized (i) and nano-sized (ii) anatase rods. The inset is plots of the transformed Kubelka–Munk function *vs.* the energy of light.

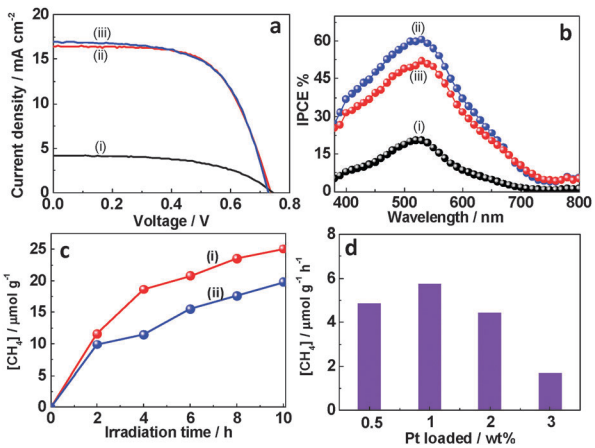

Fig. 3 (a) Photocurrent density–voltage curves and (b) action spectra of the dye-sensitized solar cells with (i) the micro-sized, (ii) nano-sized anatase rods with dominant {010} and (iii) P25 TiO_2 nanocrystals as working anodes; (c) time-dependence of photocatalytic conversion of CO_2 into CH_4 with (i) the nano-sized rods and (ii) P25 TiO_2 nanocrystals loaded with 1 wt% Pt; (d) average conversion rate of CO_2 into CH_4 for the initial 2 h with the nano-sized rods loaded with different percents of Pt cocatalyst.

(16.9 and 7.69%) of the reference electrode fabricated with the benchmark P25 TiO_2 nanocrystals, whose specific surface area is nearly two times higher than our nano-sized rods (48 *vs.* 25 $m^2\ g^{-1}$). A reasonable explanation for the good performance of the {010} dominant anatase rods can be attributed to the unique surface atomic structure featuring both 100% five-coordinated Ti (Ti_{5c}) atoms and very flat bond configurations (see Fig. 4a in ref. 4), which may contribute to the effective adsorption of dye molecules and promote electron transfer from excited molecules to TiO_2. In addition, the electrodes of the {010} dominant rods have a marginally larger open-circuit voltage V_{oc} than that of P25 as a result of their higher CB minimum (739 *vs.* 727 mV).

Photocatalytic conversion of CO_2 into chemical fuels such as CH_4 and CH_3OH is a highly important yet very challenging research topic.[13] This is largely due to the multi-carrier transfer processes required not only by the photooxidation of H_2O with holes from VB but also the photoreduction of CO_2 with electrons from CB, for instance, $CO_2 + 8e^- + 8H^+ \rightarrow CH_4 + 2H_2O$ [$E^0(CO_2/CH_4) = -0.24$ V *vs.* NHE, pH = 7]. We estimated the photocatalytic conversion activity of CO_2 into CH_4 of the Pt-loaded nano-sized {010} dominant anatase rods in the presence of H_2O vapor. The rods give a superior activity to P25 TiO_2 nanocrystals in generating CH_4 throughout the whole reaction duration of 10 h, as shown in Fig. 3c. The deviation of the CO_2 conversion rate from the linear relationship may be caused by the continuously increased concentration of CH_4 in the reaction chamber during reactions. Systematic studies on the activity dependence on the amount of Pt cocatalysts suggest that 1 wt% loading is optimal.

The excellent performance in converting CO_2 into CH_4 of the {010} dominant rods can be understood as the synergistic effects of both the unique surface atomic structure and higher CB minimum of {010}. The adsorption of reactant H_2O and CO_2 molecules on the photocatalyst surface is a prerequisite for the subsequent electron transfer and conversion reactions. Theoretically, H_2O molecules at low coverage can be dissociatively adsorbed on the (010) surface with 100% Ti_{5c} atoms, while the molecules can only be molecularly adsorbed on (101).[14a] Furthermore, the interaction of CO_2 on the (010) is predicted to be stronger than that on both (101) and (001).[14b] All these features favor the adsorption of CO_2 and H_2O on (010). Equally important, it has been experimentally verified that the photoexcited electrons in a more negative CB have a greater ability to reduce CO_2.[13a] In the current case, the electrons from a more negative CB of {010} dominant rods can effectively reduce CO_2 as indicated in Fig. 3d.

Finally, it is useful to discuss the possible growth processes of the {010} dominant TiO_2 rods from lepidocrocite-type $Cs_{0.68}Ti_{1.83}O_4/H_{0.68}Ti_{1.83}O_4$. By monitoring the crystalline structure and morphology evolution of intermediate solid products with reaction times of 0–24 h (see Fig. S5 and S6, ESI†), three typical stages can be identified for the formation of the micro-sized TiO_2 rods from $Cs_{0.68}Ti_{1.83}O_4$: (i) dissolution (0–4 h) of $Cs_{0.68}Ti_{1.83}O_4$ to increase both the concentration of soluble titanium species from nil to the critical point for TiO_2 nucleation and the aqueous pH value by releasing Cs^+; (ii) a coexistence stage (5–18 h) of $Cs_{0.68}Ti_{1.83}O_4$ and TiO_2; (iii) a possible ripening and recrystallization stage after 18 h. In stages (i) and (ii), the gradual release of titanium species and concomitant pH value increase of the solution from an initial 8.4 to a final 12.1 play a central role in controlling the nucleation and growth of TiO_2, and obtaining a high percentage of {010}. Regarding the formation processes of the nano-sized rods from $H_{0.68}Ti_{1.83}O_4$, the obvious differences from the above include a faster dissolution rate of $H_{0.68}Ti_{1.83}O_4$ than $Cs_{0.68}Ti_{1.83}O_4$ and a higher initial pH value (10.8) mediated by additional Cs_2CO_3 and slightly increased pH value (11.5) during the reaction. These features result in a much higher density of TiO_2 nucleation and consequently smaller rods. The pH value mediator Cs_2CO_3 can be replaced by other weak basic agents such as Na_2CO_3 and K_2CO_3 to prepare similar nano-sized rods (see Fig. S7, ESI†).

The authors thank NSFC (Nos. 50921004, 51002160, 21090343), Solar Energy Initiative of CAS for financial support. GL thanks the IMR SYNL-T.S. Kê Research Fellowship.

Notes and references

1 (*a*) M. R. Hoffmann, S. T. Martin, W. Choi and D. W. Bahnemann, *Chem. Rev.*, 1995, **95**, 69; (*b*) H. Tada, T. Kiyonaga and S. Naya, *Chem. Soc. Rev.*, 2009, **38**, 1849; (*c*) A. Kudo and Y. Miseki, *Chem. Soc. Rev.*, 2009, **38**, 253; (*d*) X. L. Hu, G. S. Li and J. C. Yu, *Langmuir*, 2010, **26**, 3031; (*e*) J. H. Pan, H. Q. Dou, Z. G. Xiong, C. Xu, J. Z. Ma and X. S. Zhao, *J. Mater. Chem.*, 2010, **20**, 4512; (*f*) Z. G. Zou, J. H. Ye, K. Sayama and H. Arakawa, *Nature*, 2001, **414**, 625; (*g*) K. Maeda, K. Teramura, D. L. Lu, T. Takata, N. Saito, Y. Inoue and K. Domen, *Nature*, 2006, **440**, 7082; (*h*) H. J. Yang, J. H. Yang, G. J. Ma, G. P. Wu, X. Zong, Z. B. Lei, J. Y. Shi and C. Li, *J. Catal.*, 2009, **266**, 165.
2 (*a*) W. Q. Fang, X. Q. Gong and H. G. Yang, *J. Phys. Chem. Lett.*, 2011, **2**, 725; (*b*) G. Liu, J. C. Yu, G. Q. Lu and H. M. Cheng, *Chem. Commun.*, 2011, **47**, 6763.
3 H. G. Yang, C. H. Sun, S. Z. Qiao, J. Zou, G. Liu, S. C. Smith, H. M. Cheng and G. Q. Lu, *Nature*, 2008, **453**, 638.
4 J. Pan, G. Liu, G. Q. Lu and H. M. Cheng, *Angew. Chem., Int. Ed.*, 2011, **50**, 2133.
5 (*a*) M. Lazzeri, A. Vittadini and A. Selloni, *Phys. Rev. B*, 2002, **65**, 119901; (*b*) C. T. Dinh, T. D. Nguyen, F. Kleitz and T. O. Do, *ACS Nano*, 2009, **3**, 3737.
6 J. M. Li and D. S. Xu, *Chem. Commun.*, 2010, **46**, 2301.
7 A. S. Barnard and L. A. Curtiss, *Nano Lett.*, 2005, **5**, 1261.
8 T. Sasaki, M. Watanabe, H. Hashizume, H. Yamada and H. Nakazawa, *J. Am. Chem. Soc.*, 1996, **118**, 8329.
9 G. Liu, H. G. Yang, X. W. Wang, L. N. Cheng, J. Pan, G. Q. Lu and H. M. Cheng, *J. Am. Chem. Soc.*, 2009, **131**, 12868.
10 G. Liu, C. H. Sun, H. G. Yang, S. C. Smith, L. Z. Wang, G. Q. Lu and H. M. Cheng, *Chem. Commun.*, 2010, **46**, 755.
11 B. Oregan and M. Grätzel, *Nature*, 1991, **353**, 737.
12 J. G. Yu, J. J. Fan and K. L. Lv, *Nanoscale*, 2010, **2**, 2144.
13 (*a*) T. Inoue, A. Fujishima, S. Konishi and K. Honda, *Nature*, 1979, **277**, 637; (*b*) V. P. Indrakanti, J. D. Kubick and H. H. Schobert, *Energy Environ. Sci.*, 2009, **2**, 745; (*c*) S. C. Roy, O. K. Varghese, M. Paulose and C. A. Grimes, *ACS Nano*, 2010, **4**, 1259; (*d*) Q. Liu, Y. Zhou, J. Kou, X. Chen, Z. Tian, J. Gao, S. Yan and Z. G. Zou, *J. Am. Chem. Soc.*, 2010, **132**, 14385; (*e*) S. Yan, S. Ouyang, J. Gao, M. Yang, J. Feng, X. Fan, L. Wan, Z. Li, J. H. Ye, Y. Zhou and Z. G. Zou, *Angew. Chem., Int. Ed.*, 2010, **49**, 6400; (*f*) N. Zhang, S. Ouyang, P. Li, Y. Zhang, G. Xi, T. Kako and J. H. Ye, *Chem. Commun.*, 2011, **47**, 2041.
14 (*a*) A. Ignatchenko, D. G. Nealon, R. Dushane and K. Humphries, *J. Mol. Catal. A: Chem.*, 2006, **256**, 57; (*b*) V. P. Indrakanti, J. D. Kubicki and H. H. Schobert, *Energy Fuels*, 2008, **22**, 2611.